

**EXPERIMENTAL INVESTIGATION ON THE  
FLOW STRUCTURE OF A HYBRID TURBINE  
BLADE FOR HYDROKINETIC APPLICATION**

**NURUL ASYIKIN BINTI ABU BAKAR**

**SCHOOL OF AEROSPACE ENGINEERING  
UNIVERSITI SAINS MALAYSIA**

**2021**

**EXPERIMENTAL INVESTIGATION ON THE FLOW STRUCTURE OF A  
HYBRID TURBINE BLADE FOR HYDROKINETIC APPLICATION**

**by**

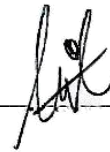
**NURUL ASYIKIN BINTI ABU BAKAR**

**Thesis submitted in fulfilment of the requirements for the  
Bachelor degree of Engineering (Honours) (Aerospace Engineering)**

**June 2021**

## ENDORSEMENT

I, Nurul Asyikin Binti Abu Bakar hereby declare that I have checked and revised the whole draft of dissertation as required by my supervisor.



(Signature of Student)

Date: 27 June 2021



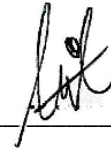
(Signature of Supervisor)

Name: Dr Noorfazreena M. Kamaruddin

Date: 27 June 2021

## ENDORSEMENT

I, Nurul Asyikin Binti Abu Bakar hereby declare that all corrections and comments made by the supervisor and examiner have been taken consideration and rectified accordingly.



(Signature of Student)

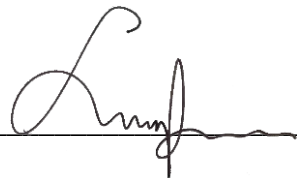
Date: 8 July 2021



(Signature of Supervisor)

Name: Dr Noorfazreena M. Kamaruddin

Date: 8 July 2021



(Signature of Examiner)

Name: Dr. Norizham Bin Abdul Razak

Date: 9/7/2021

## DECLARATION

This thesis is the result of my own investigation, except where otherwise stated and has not previously been accepted in substance for any degree and is not being concurrently submitted in candidature for any other degree.



---

(Signature of Student)

Date: 8 July 2021

## **ACKNOWLEDGEMENTS**

I would like to address my deepest gratitude to my final year project supervisor, Dr. Noorfazreena Kamaruddin for her guidance on this journey. Her advice and patience guided me through this final year project, as well as my undergraduate studies at Universiti Sains Malaysia (USM), able to motivate me to complete this project. I am also honored to be part of the final year project under her supervision where lots of learning and the deepest knowledge are applied in the process of understanding the flow behavior around the turbine. Her precious effort and continuous supportive motivation in the critical process were able to encourage me to stay on the path and complete this project that without her valuable support, this dissertation would not have been possible.

Furthermore, I would like to address my thanks to the school's staff, En Zulhairi for his help in fabricating the endplates and En. Najhan for his help in providing equipment in the wind tunnel lab. Next, I would like to thank En. Najib for his hospitality in providing the materials and equipment in the assembly process. Next, I would like to express my thanks to Badrul and Syukri for their help in the fabricating process and assisted me in the experimental set-up to ensure the project was carried out in an efficient and safe environment. I would like to also thank my fellow friends and seniors for their support and advice on this project.

Finally, I would like to thank the University for providing with all of the equipment and facilities needed to complete this project. I would expand appreciation of my grateful feeling to my family members by supporting and motivating me, especially my parents during my undergraduate studies.

# EXPERIMENTAL INVESTIGATION ON THE FLOW STRUCTURE OF A HYBRID TURBINE BLADE FOR HYDROKINETIC APPLICATION

## ABSTRACT

The hydrokinetic turbine has emerged as an alternative method for rural communities to generate energy for daily needs and to improve their living conditions. Due to the current pandemic, daily energy requirements in education are increasing, shifting from face-to-face learning to an online platform. This study aims to fabricate a hybrid turbine and analyze the flow behavior around the turbine that affects the power performance for the hydrokinetic application at various incoming flow speeds,  $V_\infty$ . The proposed hybrid turbine was designed by combining the two vertical axis turbines; Savonius and Darrieus turbines to overcome their respective disadvantages, as the Savonius turbine has a low power performance, while the Darrieus turbine has a low self-starting speed. The performance of the hybrid turbine is evaluated by analyzing the flow behavior around it, as well as the data on the coefficients of torque and power with respect to the tip speed ratio value. The hybrid turbine was tested in a closed-circuit wind tunnel at various flow speeds,  $V_\infty=4, 5, 6, \text{ and } 7 \text{ m/s}$ , to represent the typical river speed in Malaysia with Reynolds numbers of 89500, 112000, 134000, and 157000. The results showed that at the highest Reynolds number of 157000 the hybrid turbine has a strong flow attachment, resulting in the smallest wake size. At a higher Reynolds number, the flow separation is also delayed, resulting in a smaller recirculation region behind the turbine. The hybrid turbine shows an increase in power coefficient at the highest Reynold number of 157000 with 0.17 at a tip speed ratio of 0.66. Based on this, the hybrid turbine has the potential to be implemented for hydrokinetic applications and contribute to higher rates of electrification in Malaysia's rural communities, particularly in Sabah and Sarawak.

# **KAJIAN EKSPERIMEN PADA STRUKTUR ALIRAN BILAH TURBIN HIBRID UNTUK APLIKASI HIDROKINETIK**

## **ABSTRAK**

Turbin hidrokinetik telah muncul menjadi kaedah alternatif bagi masyarakat luar bandar untuk menjana tenaga untuk keperluan harian untuk memperbaiki keadaan hidup mereka. Oleh kerana keadaan pandemic semasa, keperluan tenaga harian dalam pendidikan semakin beralih dari pembelajaran tatap muka ke platform dalam talian. Kajian ini bertujuan untuk membuat turbin hibrid dan menganalisis tingkah laku aliran di sekitar turbin yang mempengaruhi prestasi daya untuk aplikasi hidrokinetik pada pelbagai kelajuan aliran masuk,  $V_{\infty}$ . Turbin hibrid yang dicadangkan adalah dengan menggabungkan dua turbin paksi menegak; Turbin Savonius dan Darrieus untuk mengatasi kekurangan masing-masing, kerana turbin Savonius mempunyai prestasi daya rendah, sementara turbin Darrieus mempunyai kelajuan permulaan diri yang rendah. Prestasi turbin hibrid dinilai dengan menganalisis tingkah laku aliran di sekitarnya, serta data mengenai pekali tork dan daya berkenaan dengan nilai nisbah kelajuan hujung. Turbin hibrid diuji dalam terowong angin litar tertutup pada pelbagai kelajuan aliran,  $V_{\infty} = 4, 5, 6, \text{ dan } 7 \text{ m/s}$ , untuk mewakili kelajuan sungai khas di Malaysia dengan bilangan Reynolds 89500, 112000, 134000, dan 157000. Hasil kajian menunjukkan bahawa pada jumlah Reynolds tertinggi 157000 turbin hibrid mempunyai lampiran aliran yang sangat kuat, menghasilkan saiz bangun terkecil. Nombor Reynolds yang lebih tinggi, pemisahan aliran juga ditangguhkan sehingga menghasilkan kawasan peredaran semula yang lebih kecil di belakang turbin. Turbin hibrid menunjukkan peningkatan pekali kuasa pada bilangan Reynold tertinggi 157000 dengan 0.17 pada nisbah kelajuan tip 0.66. Berdasarkan ini, turbin hibrid berpotensi dilaksanakan untuk aplikasi



hidrokinetik dan menyumbang kepada kadar elektrik yang lebih tinggi di masyarakat luar bandar Malaysia, terutama di Sabah dan Sarawak.

## TABLE OF CONTENT

<b>ENDORSEMENT</b>	<b>I</b>
<b>ENDORSEMENT</b>	<b>II</b>
<b>DECLARATION</b>	<b>III</b>
<b>ACKNOWLEDGEMENTS</b>	<b>IV</b>
<b>ABSTRACT</b>	<b>V</b>
<b>ABSTRAK</b>	<b>VI</b>
<b>TABLE OF CONTENT</b>	<b>VIII</b>
<b>LIST OF FIGURES</b>	<b>X</b>
<b>LIST OF TABLES</b>	<b>XIII</b>
<b>LIST OF ABBREVIATIONS</b>	<b>XIV</b>
<b>LIST OF SYMBOLS</b>	<b>XIV</b>
<b>CHAPTER 1</b>	<b>1</b>
1.1 Overview	1
1.2 Motivation and Problem Statement	2
1.3 Objectives	4
1.4 Thesis outline	4
<b>CHAPTER 2</b>	<b>7</b>
2.1 Types of Hydrokinetic Turbine	8
2.1.1 Lift-Driven Turbine.	9
2.1.2 Drag-Driven turbine	11
2.1.3 Hybrid Turbine	12
2.2 Airfoil selection	14
2.3 Flow visualization techniques.	17
2.4 Relevance of previous literature to the current study	24
2.4.1 Hybrid turbine selection	24
2.4.1 Flow visualization method	26
<b>CHAPTER 3</b>	<b>28</b>
3.1 Hybrid Turbine Model Design and Fabrication	29
3.2 Fabrication process.	30
3.3 Experimental setup	32
3.4 Flow visualization set up.	34
3.5 Torque measurement set up.	36
3.6 Data reduction	37
3.7 Uncertainty analysis	39

<b>CHAPTER 4</b>	<b>41</b>
4.1 The flow parameter	42
4.2 Flow visualization of the hybrid turbine.	42
4.3 The coefficient of power, $C_P$ , and the coefficient of torque, $C_T$ of the hybrid turbine.	45
<b>CHAPTER 5</b>	<b>51</b>
5.1 Conclusion	51
5.2 Recommendation	53
<b>REFERENCES</b>	<b>55</b>
<b>APPENDICES</b>	<b>61</b>
6.1 Data acquisition at 4 m/s	61
6.2 Data acquisition at 5 m/s	62
6.3 Data acquisition at 6 m/s	63
6.4 Data acquisition at 7 m/s	64
6.5 Uncertainty Analysis calculation at the highest power coefficient, $C_P$	66

## LIST OF FIGURES

Figure 1.1: The electricity generation in Malaysia. (Suruhanjaya Tenaga, 2019)	2
Figure 1.1: The river network of Sarawak (Ministry of Environment and Water, 2017)	3
Figure 1.3: The river network of Sabah (Ministry of Environment and Water, 2017).	3
Figure 2.1: The overview of the literature review section	7
Figure 2.2: The Power Coefficient with the Tip Speed Ratio (Frank R. Eldridge, 1980).	8
Figure 2.3: Horizontal axis turbine ( <i>Horizontal axis wind turbine wind generator blue</i> , 2020).	9
Figure 2.4: The Darrieus turbine (Kirke and Lazauskas, 2011)	10
Figure 2.5: The operation of the Darrieus turbine (Kumara et al. 2017)	11
Figure 2.6: 2-Stages of Savonius Turbine ( <i>Vertical Wind Generator 240 W elvwis</i> ® <i>III Aluminium + Bracket Wind Turbine VAWT</i> , 2021)	12
Figure 2.7: The operation of Savonius turbine (Salleh et al. 2019)	12
Figure 2.8: The hybrid turbine in 2 stages (Gupta and Sharma, 2012).	13
Figure 2.9: The single-stage hybrid turbine with different blades' radius (Sahim et al. 2018).	14

Figure 2.10: The lift to drag ratio against the angle of attack of the airfoils. (Alsabri et al. 2019)	17
Figure 2.11: The visualization of the set-up of the PIV method with the connected apparatus. (Neeraj and Lal, 2014)	19
Figure 2.12: The PIV flow visualization at each rotor position (Dobrev and Massouh, 2012)	20
Figure 2.13: The velocity contour of time average stream-wise velocity (Rolin and Porté-Agel, 2015).	20
Figure 2.14: The smoke lines around the Savonius turbine (Fujisawa and Gotoh, 1992)	22
Figure 2.15: The type of smoke oils tested in the wind tunnel (Shamsuddin and Kamaruddin, 2020)	23
Figure 2.16: The Illumination system's light to show the smoke lines (Shamsuddin and Kamaruddin, 2020)	24
Figure 3.1: Overview of methodology	28
Figure 3.2: (a) The Solidwork model design and (b) the assembly of the fabricated Hybrid Turbine Model.	30
Figure 3.3: The 3D printing setting.	32
Figure 3.4: The printing parts in Ultimaker Cura.	32
Figure 3.5: The location of the hybrid turbine in the test section.	33
Figure 3.6: The side view of the hybrid turbine in the test section.	33

Figure 3.7: The flow visualization setup.	34
Figure 3.8: The setup of the flow visualization experiment at the top of the wind tunnel test section.	35
Figure 3.9: The side view setup of the flow visualization experiment.	35
Figure 3.10: (a) The Prony dynamometer setup and (b) The torque experiment setup	36
Figure 3.11: The Prony dynamometer setup.	37
Figure 4.1: The overview of the result and discussion.	41
Figure 4.2: The Instantaneous flow structures around the hybrid turbine at the various of incoming flow speed, $V_{\infty}$	44
Figure 4.3: The performance of the hybrid turbine.	46
Figure 4.4: Comparison of the Hybrid Turbine power performance of the previous study with the present study.	49

## LIST OF TABLES

Table 2.1: The turbine type and its axis of rotation.	9
Table 2.2: The power coefficient of the airfoils (Mohamed, 2012a)	15
Table 2.3: The flow visualization technique with the range of speed and the medium of the techniques (Wolfgang, 1987)	18
Table 2.4: The smoke liquid properties (Trinder and Jabbal, 2013; Shamsuddin and Kamaruddin, 2020)	23
Table 2.5: The turbine selection with its advantages and disadvantages.	25
Table 2.6: The Lift-to-Drag ratio value of the airfoil.	26
Table 2.7: The smoke generator system parameters.	27
Table 3.1: The dimension of the hybrid turbine and the important physical design parameter of the hybrid turbine.	30
Table 3.2: The fabrication process of all parts of the hybrid turbine model.	31
Table 3.3: The important parameters of the 3D printing process.	31
Table 3.4: The values of uncertainty percentage of the important parameters of the experiment.	40
Table 4.1: The values of Reynolds number and velocity	42
Table 4.2: The performance of the hybrid turbine parameter at the maximum power coefficient, $C_p$ .	47
Table 4.3: The comparison data of the Reynolds number with the previous study and present study of the hybrid turbine.	48

## LIST OF ABBREVIATIONS

HKT	: Hydrokinetic turbine
RPM	: Revolution per minute

## LIST OF SYMBOLS

### *Latin symbols*

$AR$	: Aspect ratio
$BR$	: Blockage ratio
$C_P$	: Coefficient of power
$C_{Pmax}$	: Maximum coefficient of power
$C_T$	: Coefficient of torque
$D$	: Diameter of the turbine (m)
$D_S$	: Diameter of the Savonius rotor (m)
$D_D$	: Diameter of the Darrieus rotor (m)
$D_E$	: Diameter of the endplate (m)
$d$	: Diameter of blade (m)
$d_s$	: Diameter of shaft (m)
$e$	: Overlap distance (m)
$ER$	: Endplate ratio
$F_1$	: Load acquired by load cell 1 (N)
$F_2$	: Load acquired by load cell 2 (N)
$H$	: Height of turbine (m)
$h$	: Height of the test section (m)
$h_d$	: Height of deflector (m)



$l$	: Length of the test section (m)
$n$	: Number of blades
$OR$	: Overlap ratio
$R$	: Radius of the turbine (m)
$Re$	: Reynolds number
$RL$	: Radius ratio
$R_S$	: Radius of the Savonius rotor (m)
$R_D$	: Radius of the Darrieus rotor (m)
$r_p$	: Radius of pulley (m)
$T$	: Dynamic torque (Nm)
$t_b$	: Thickness of blade (m)
$t_E$	: Thickness of end plate (m)
$V_\infty$	: Fluid flow speed (m/s)
$w$	: Width of the test section (m)

***Greek symbols***

$\lambda$	: Tip speed ratio
$\mu$	: Dynamic viscosity of fluid (kg/ms)
$\rho$	: Density of fluid (kg/m <sup>3</sup> )
$\omega$	: Angular velocity (rad/s)

# CHAPTER 1

## INTRODUCTION

### 1.1 Overview

The high demands for electrical usage in Asia are increasing rapidly compared to other regions in the world (EIA, 2019). Currently, the majority of energy produced is derived from petroleum and coal, both of which are in short supply. With this major energy generated by burning petroleum, carbon dioxide emissions will continue to rise, contributing to global climate change. Renewable energy sources, such as solar, wind, and hydropower are becoming more prevalent in developing countries. Renewable energy has low environmental effects on the flora and fauna. The development of renewable energy is still ongoing, with more people experimenting and improvising with this type of renewable energy. Most research aims to produce high power so that it can replace non-renewable energy resources.

Malaysia is one of the countries that uses coal as a non-renewable energy source, accounting for 50.6% of the total energy generated (Suruhanjaya Tenaga, 2019). In comparison to wind and solar power, hydropower has grown due to its high reliability in generating energy in Malaysia's weather and climate. Wind energy is expected to reduce carbon dioxide emissions by about 3 billion tonnes by 2030 (Ritchie and Roser, 2017). However, wind energy requires large areas with high wind speed, and Malaysia's unpredictable weather may not be able to meet the high demand because the average wind speed is relatively low ranging from 1.5 to 4.5 m/s (M. S. N. Samsudin, M. M. Rahman, 2016). Solar power may also not provide the best performance in Malaysia because the weather during the monsoon season will be difficult for the solar panels to be exposed to the sun. The solar power source may be beneficial to the rural community

population. However, it has the highest installation maintenance cost (Mekhilef *et al.*, 2012). The estimated return on investment for solar PV systems is about 8.7 years (Wei and Saad, 2020). The use of hydropower could help to increase the percentage of usage of renewable energy. The hybrid turbine may be the most practical choice for the hydrokinetic application due to its low manufacturing cost, low environmental impact, and high efficiency as the water is denser than air (Hossain *et al.*, 2015).

Renewable energy sources, such as solar, wind, and hydropower are becoming more common in developing countries. Figure 1.1, shows that of the three renewable energy developments in Malaysia, hydropower energy has grown the most from 6.7% in 1999 to 16.6% in 2017 (Suruhanjaya Tenaga, 2019).

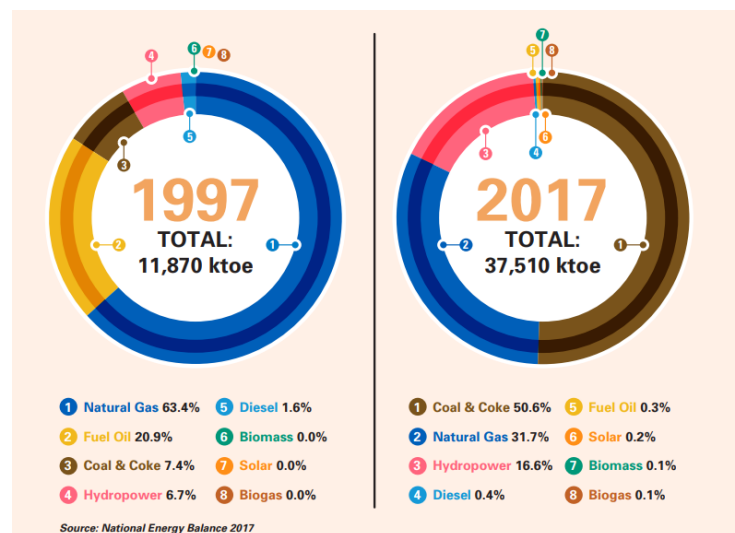


Figure 1.1: The electricity generation in Malaysia. (Suruhanjaya Tenaga, 2019)

## 1.2 Motivation and Problem Statement

As Malaysia is a developing country, there are some isolated areas in Peninsular Malaysia that do not have access to electricity. The states of Sabah and Sarawak, for example, have fewer rural communities with the electrification rates of about 77% and 67%, respectively (Rahim *et al.* 2012). This is due to the dense forest and difficult terrain



The motivation of the current study is to investigate and understand the flow behavior around a hybrid turbine at various incoming flow, velocities,  $V_{\infty}$  as it relates to the recirculation flow produced by the hybrid turbine. As a result, the power performance of the hybrid turbine is influenced by the flow characteristics. It is critical to use proper visualization to clearly show the streamlines and capture the flow characteristics. The flow behavior around the rotating turbine must be described and analyzed because it has a significant impact on hybrid turbine performance when used in typical Malaysia's river flow. This study is part of an effort to contribute to improve the rural electrification program in Malaysia (Kementerian Pembangunan Luar Bandar, 2020) as the micro-hybrid turbine is one of the alternative resource methods to independently generate energy and distribute it to rural communities that do not have access to the national grid network, particularly in Malaysia's Borneo.

### **1.3 Objectives**

The objective of this study is:

- To investigate the flow behavior around the hybrid turbine and analyze its performance.

### **1.4 Thesis outline**

This thesis is divided into several chapters. Chapter one introduces the renewable energy with the motivation to contribute to renewable energy development in Malaysia.

The objective of this study is also listed in the first chapter to outline the purpose of this study.

The second chapter is a review of the literature on the various types of turbines available and their performance in the previous study. This review aided in the selection of the turbine type for use in modelling the hybrid turbine in this study. The flow condition from the previous study was also reviewed and analyzed to understand the flow state and the boundary condition of the rotating object. This chapter lists flow visualization techniques to analyze the best visualization method with the appropriate medium and the condition of the hybrid turbine.

Chapter 3 consists of the methodology for modelling and fabrication of the hybrid turbine along with the fabrication process for each component of the hybrid turbine. This chapter also explains the setup of both qualitative and quantitative measurements. The flow visualization technique chosen is discussed in conjunction with the position of the setup to achieve the best quality result. The torque measurement setup is also required in order to obtain the torque value data to validate the hybrid turbine performance.

Chapter 4 discusses on the results of the qualitative and quantitative measurements that includes the discussion of turbine performance in relation to the flow behavior with under various flow conditions. The important parameters of the hybrid turbine discussed in this section are the coefficient of power, the coefficient of torque and the tip speed ratio, as well as the aerodynamic flow visualization after the incoming flow hits the turbine.

The last chapter summarizes the findings of this study as well as the overall important points of flow behavior around the hybrid turbine that affect its performance.

This chapter also discusses the recommendations and improvements that could be made to the hybrid turbine.

## CHAPTER 2

### LITERATURE REVIEW

A literature review was conducted on various types of turbines to determine the turbine capability under specific conditions that are best for the turbine type in order to generate the best model combination of both lift and drag-driven turbines as shown in Figure 2.1. The hybrid turbine performance from the previous studies was also reviewed using various designs and parameters. The review of the airfoil in the lift-driven turbine was also included in this section to estimate the lift to drag ratio, which generates more lift to rotate the turbine. The flow visualization techniques to determine the best method to illustrate the flow around the hybrid turbine are as also discussed in this section.

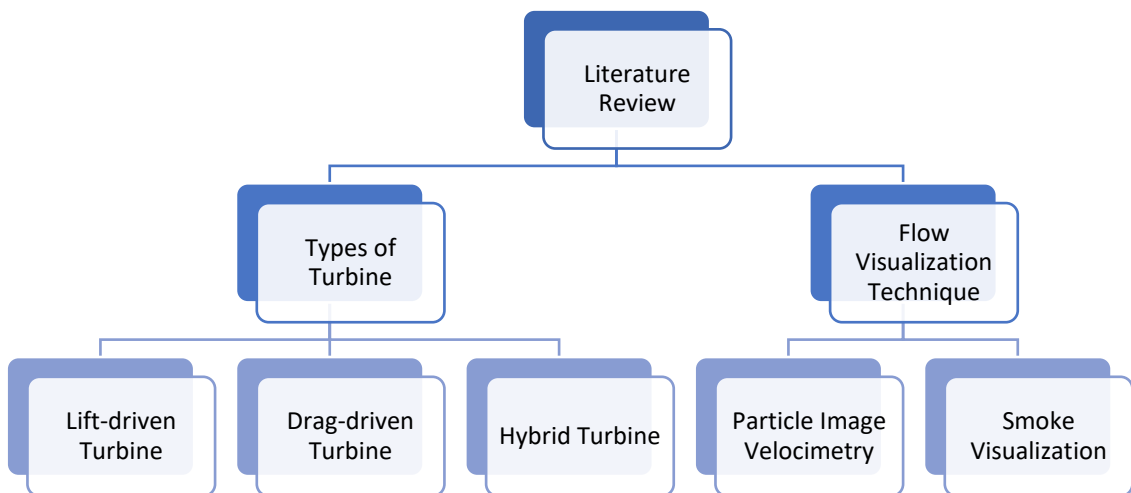


Figure 2.1: The overview of the literature review section



## 2.1 Types of Hydrokinetic Turbine

The flow structure of the blade will influence the performance of the hybrid turbine. As a result, this study examines various types of hydrokinetic turbines. The turbine is also divided into a horizontal axis and a vertical axis that depends on the rotation (Goldstein, 2015). The hydrokinetic turbine is classified as a lift-driven turbine and a drag-driven turbine (Chen *et al.*, 2015). The lift-driven turbine works because of the large velocity difference that causes to the pressure to generate lift and the rotor to rotate. While the drag-driven turbine is the flow separation from the adverse pressure gradient and drives the rotor to rotate (Hyams, 2012). The hybrid hydrokinetic is a combination of lift and drag driven by the turbine to maximize the performance of the hydrokinetic turbine. The various types of turbine performance are represented in the power coefficient in relation to the tip speed ratio is shown in Figure 2.2 (Salleh *et al.* 2019).

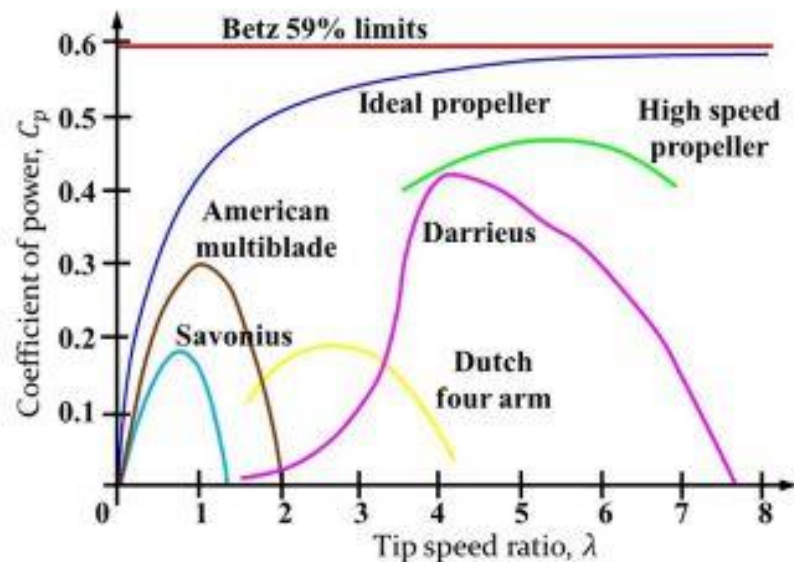


Figure 2.2: The Power Coefficient with the Tip Speed Ratio (Frank R. Eldridge, 1980).

Table 2.1: The turbine type and its axis of rotation.

Type of turbine	Axis of Rotation	Turbine Driven Force
Horizontal axis turbine	Horizontal axis	Lift-driven
Darrieus turbine	Vertical axis	Lift-driven
H-Darrieus	Vertical axis	Lift-driven
Savonius Turbine	Vertical axis	Drag-driven

### 2.1.1 Lift-Driven Turbine.

#### I. Horizontal Axis Turbine

The horizontal axis turbine shows better power efficiency as the turbine is lift-driven (Amin, 2013). The flow on the airfoil surface at the upper and lower of the airfoil surface has different pressure values and will create a force to drive the turbine rotation (M. Saad, 2014). The turbine needs to face the flow direction for high efficiency and be able to maximize the power generation. In this condition, the turbine needs the yaw mechanism in the system to face perpendicularly to the incoming flow (Wahab et al. 2004). Figure 2.3 shows the higher power coefficient in the ideal propeller in which, the turbine is able to achieve a power coefficient of 0.5.



Figure 2.3: Horizontal axis turbine (*Horizontal axis wind turbine wind generator blue*, 2020).

## II. Darrieus Turbine and H – Darrieus Turbine

The Darrieus turbine is a vertical axis turbine as the rotation axis of the turbine is on the vertical axis and the turbine is lift-driven. The turbine uses the pressure difference between both the upper and lower airfoil surfaces to rotate the turbine. The incoming flow to operate the Darrieus turbine is flexible in any direction (Kirke and Lazauskas, 2011). From Figure 2.1, the Darrieus turbine can achieve a power coefficient of 0.4 with a high tip speed ratio range. The Darrieus turbine has a higher self-starting speed due to the lower starting torque (Kirke and Lazauskas, 2011). The Darrieus turbine in Figure 2.4 shows the turbine blades with a topo-skein shape and the straight airfoil blade in Figure 2.5. The topo-skein shape blade has a lower bending momentum, resulting in high strength of the blade and higher resistance to fatigue failure with the force able to be distributed equally at the tip of the blade. The H-Darrieus in Figure 2.5 with the straight airfoil shape has a higher bending momentum at the tip of the blade due to the high centrifugal force, resulting in a lower blade strength (Moh. Magedi and Norzelawati, 2014).

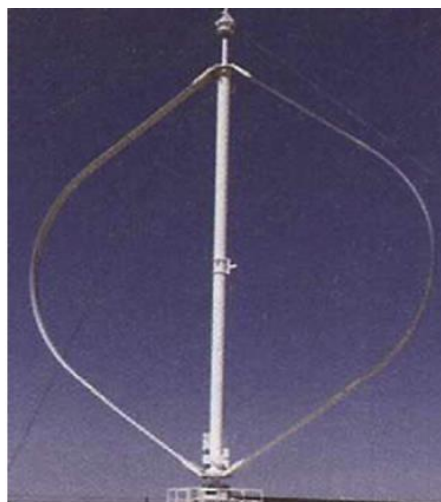


Figure 2.4: The Darrieus turbine (Kirke and Lazauskas, 2011).

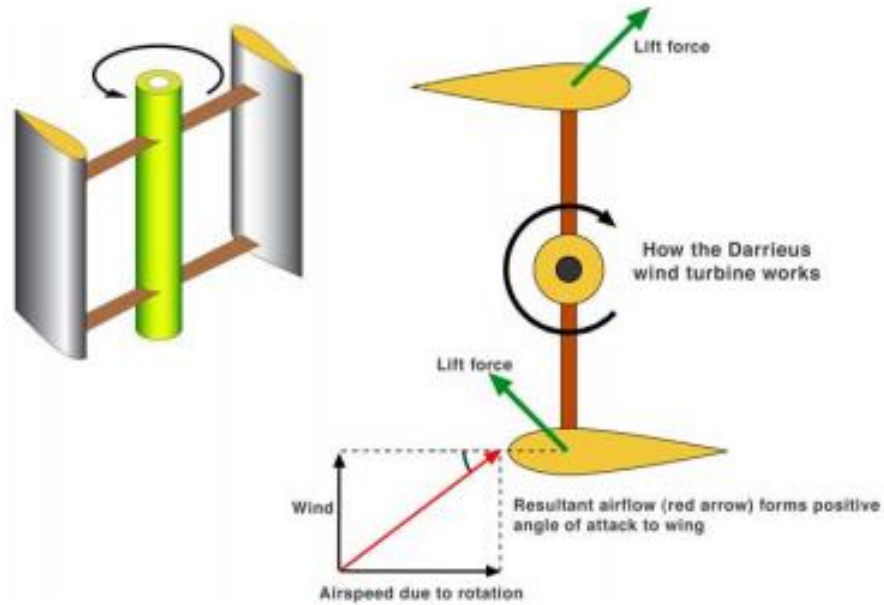


Figure 2.5: The operation of the Darrieus turbine (Kumara *et al.* 2017)

### 2.1.2 Drag-Driven turbine

#### I. Savonius Turbine.

The Savonius turbine shown in Figure 2.6 is well known for its high efficiency in low-speed flow. The turbine was able to self-start at a lower speed due to the higher torque coefficient this turbine could generate (Kumara *et al.* 2017). The turbine was able to operate in any direction of the incoming flow (Kumar and Saini, 2016). The turbine has the disadvantage of generating a higher power coefficient than the other types of turbines shown in Figure 2.1. As a result of this issue, the major research aims to improve aspects related to this type of turbine power performance. One of the improvements in the Savonius turbine is the addition of the deflector plate to channel the flow into the advancing blade, as shown in Figure 2.7 (Salleh *et al.*, 2019).



Figure 2.6: 2-Stages of Savonius Turbine (*Vertical Wind Generator 240 W elvwis ® III Aluminium + Bracket Wind Turbine VAWT*, 2021)

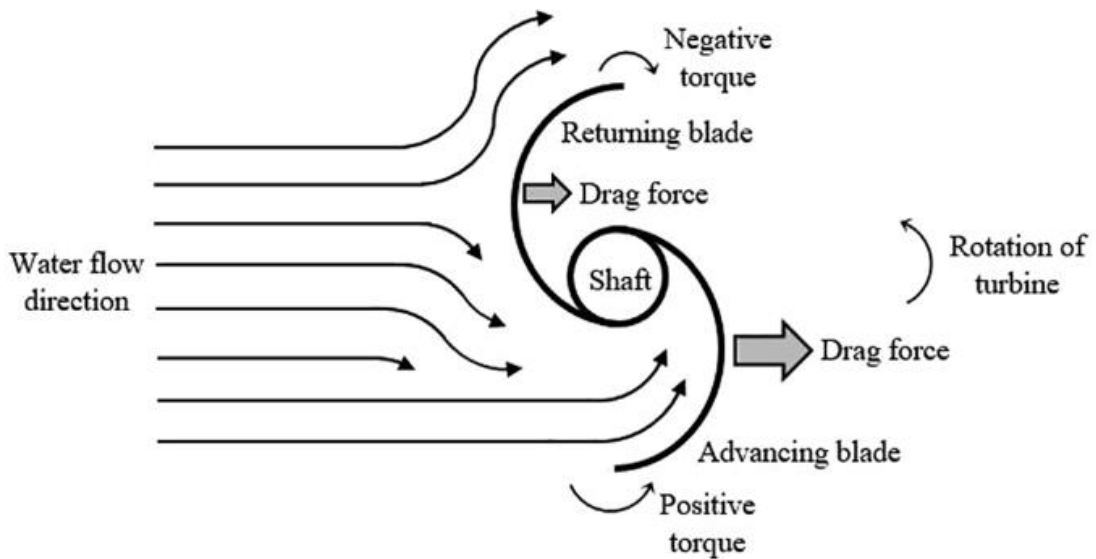


Figure 2.7: The operation of Savonius turbine (Salleh *et al.* 2019)

### 2.1.3 Hybrid Turbine

The combination of the Savonius and the drag-driven, as well as the Darrieus and the lift-driven turbine, are able to complement each other and overcome the drawbacks of both turbines. The Savonius turbine has better efficiency in operating at low-speed flow as the turbine is able to generate a high starting torque value from the drag force (Kumar and Saini, 2016). Many studies focus on improving the Savonius turbine performance due to its lower power coefficient will give great advantages as the Savonius

has better efficiency operation. As the Darrieus blade faces poor self-starting due to the low starting torque coefficient (Kirke and Lazauskas, 2011), by combining both types of turbine will produce a hybrid turbine. Then the various geometric parameter details of the hybrid turbine could be tested to achieve high performance with a better starting torque value. From Gupta and Sharma, (2012) studies on the 3 Savonius blades and 3 Darrieus blades have improved the power coefficient of 0.53 at a tip speed ratio of 0.61 with the hybrid turbine is a 2 stage combination as shown in Figure 2.8 below.

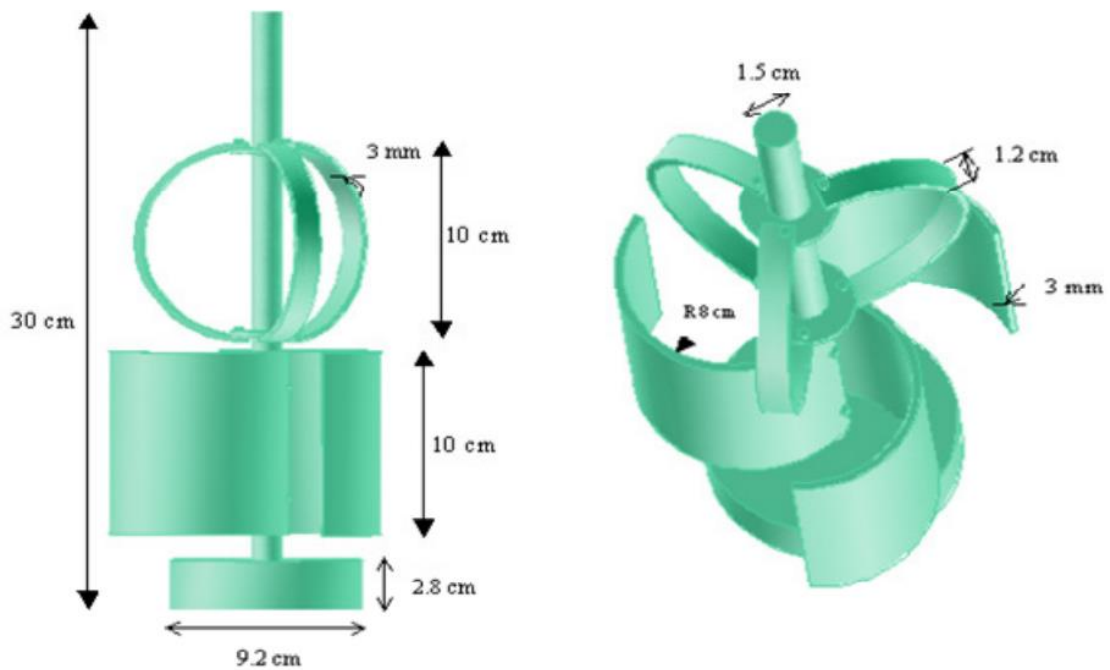


Figure 2.8: The hybrid turbine in 2 stages (Gupta and Sharma, 2012).

Another type of study was conducted using hybrid performance (Sahim et al. 2018) with 2 Savonius turbine blades and 2 Darrieus turbine blades in a single stage. The turbine achieved a coefficient of power of 0.20 at a tip speed ratio of 1.10 with a starting torque coefficient of around 0.9 at a tip speed ratio of 0.1. This turbine has a radius ratio of 0.302 with Savonius blade's radius is much smaller than the Darrieus blade's radius.

The radius of the ratio is calculated by dividing the Savonius blade radius,  $R_S$  value with the Darrieus Blade radius,  $R_D$  value illustrated in Figure 2.9.

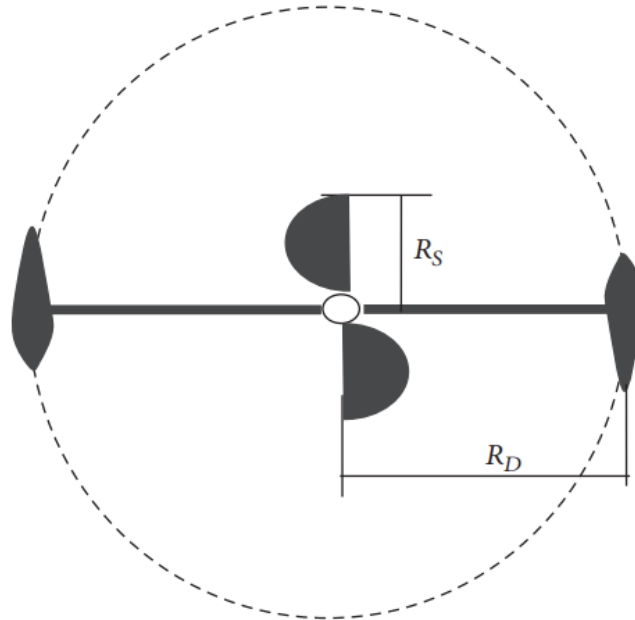


Figure 2.9: The single-stage hybrid turbine with different blades' radius (Sahim et al. 2018).

## 2.2 Airfoil selection

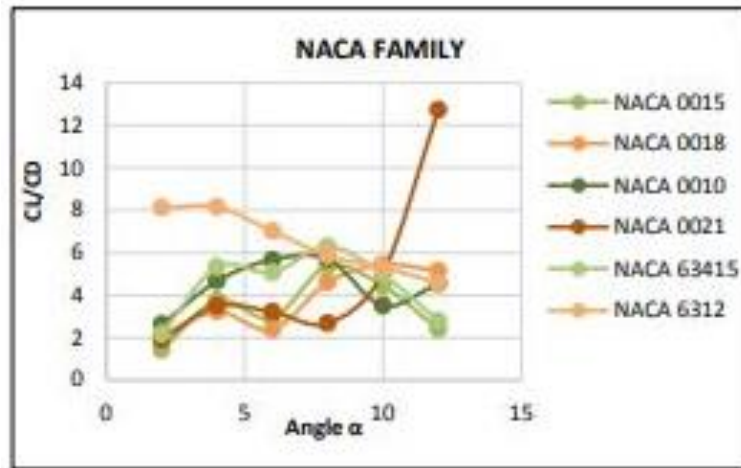
The most commonly used NACA used in the Darrieus turbine is the symmetrical airfoil, NACA 0021. From the literature, a new family of airfoils has been introduced to produce the best performance (Mohamed, 2012). The study compares the power and torque coefficients of the lift and drag forces generated from the airfoils.

Table 2.2: The power coefficient of the airfoils (Mohamed, 2012)

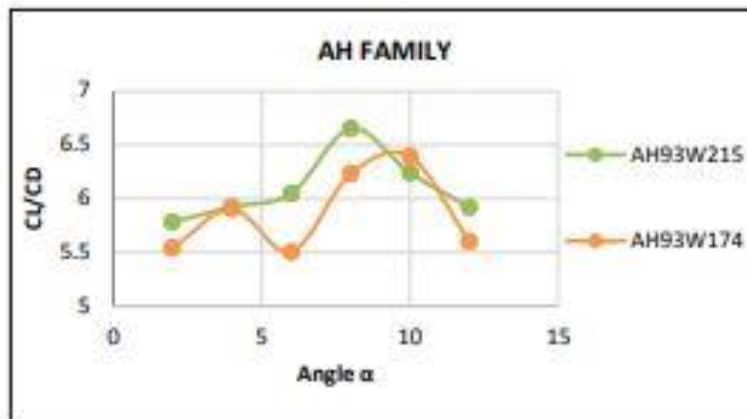
Types Of Airfoils	Power Coefficient, Cp
<b>NACA SYMMETRICAL AIRFOIL</b>	
NACA 0010	0.2345
NACA 0015	0.2947
NACA 0018	0.2964
NACA 0021	0.2679
<b>NACA NO- SYMMETRIC AIRFOIL</b>	
NACA 6312	0.1290
NACA 63415	0.171
NACA 63418	0.2772
<b>A-SERIES TYPE</b>	
AG18	0.01233
AH93W174	0.2469
AH93W215	0.2541
AH94W30	0.2130
<b>S-SERIES TYPE</b>	
S-809	0.3428
S-9000	0.1696
S-1046	0.4051
S-1014	0.2769
<b>FX-SERIES TYPE</b>	
FX66S196	0.2074
FX77W256	0.1639
FX71L150	0.2961
FXL142	0.3311
FXLV152	0.3576

The best airfoil as indicated by the best power coefficient in Table 2.2 is the S1046 with a power coefficient of 0.4051. In another study, it compared the performance of the airfoil to the lift-to-drag ratio. The highest the lift-to-drag ratio, the better the performance as the lift forces are greater than the drag forces in the flow. The lift to drag ratio is represented in the graph as below:

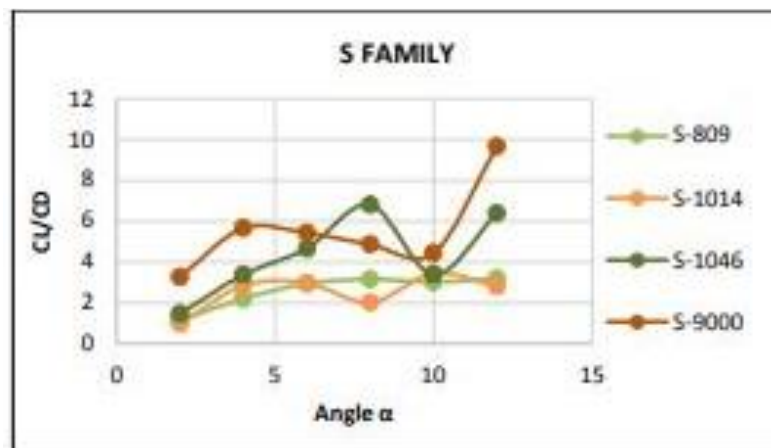




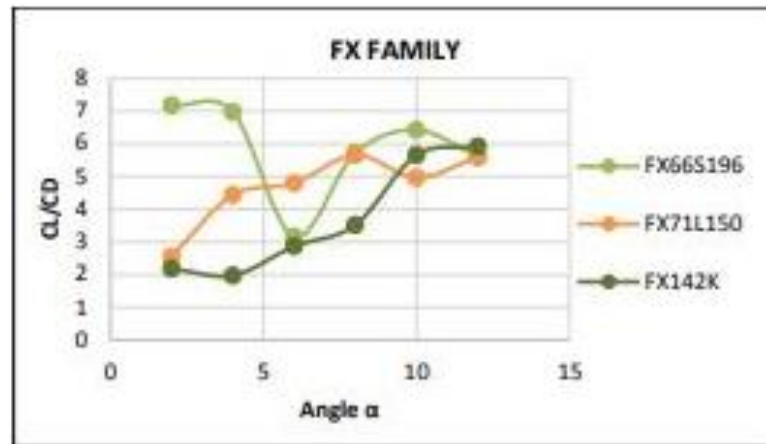
(a)Naca Symmetrical Type



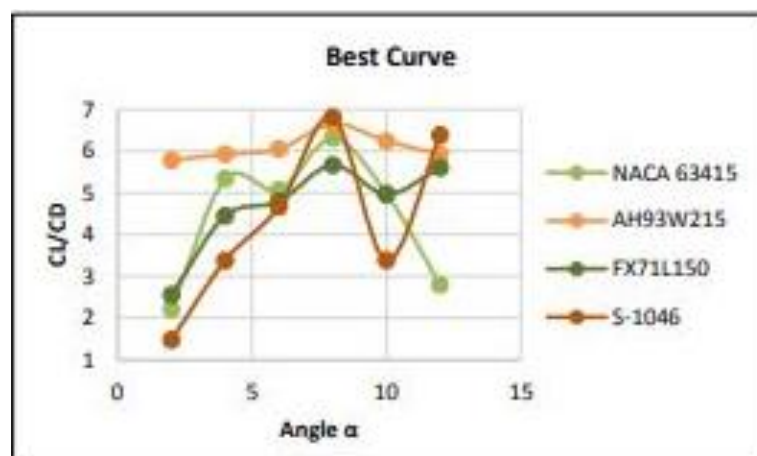
(b) A-Series Type



(c) S-Series Type



(d) FX-Series Type



(e) The of from each type of airfoil.

Figure 2.10: The lift to drag ratio against the angle of attack of the airfoils. (Alsabri et al. 2019)

The best airfoils in the graph are the A-series AH93W215 with a  $Cl/Cd$  of around 6.70 as shown in Figure 2.10. The airfoil is chosen to be the best airfoil in the turbine as it exhibits constant  $Cl/Cd$  value across the angle of attack, especially at low angle of attack value as in this study, the Darrieus airfoil at  $0^\circ$  angle of attack to the flow direction.

### 2.3 Flow visualization techniques.

In the flow visualization method, various techniques could be implemented to investigate the flow structure of the hybrid hydrokinetic turbine. The flow visualization

study is important to detect the presence of vortices behind the turbine's surrounding. Based on the literature review, good flow visualization at low speed will be able to give better results in flow visualization surrounding the hydrokinetic turbine.

Table 2.3: The flow visualization technique with the range of speed and the medium of the techniques (Wolfgang, 1987)

<b>Flow Visualization Techniques</b>	<b>Range of Speed</b>
<b>Water Medium</b>	
Dye Injection	Low Speed
Particle Image Velocimetry	Low to High Speed
<b>Air Medium</b>	
Particle Image Visualization	Low Speed
Smoke Visualization	Low Subsonic Speed
Tuft	Low Subsonic Speed
Holographic And Interferometry	Low Subsonic Speed
Shadow Graphs	Compressible Flow
Schlieren Imaging	Supersonic Speed
<b>Water And Air Medium</b>	
Wake Imaging	Low To Moderate Speed

The flow in this study focuses on the air medium with low-velocity conditions in the range of 4 m/s to 7 m/s. The test section of the experiment was in the closed-circuit wind tunnel. Thus, the air medium flow visualization technique with a low range of velocity speed is reviewed in this part.

## I. The Particle Image Velocimetry (PIV) method

Particle Image Velocimetry, (PIV) is a quantitative method to measure the behavior. This method uses scattering particles which will be added into the flow and illustrated by the light sheet and a high-speed camera to capture the flow structure (Neeraj and Lal, 2014). Figure 2.11 shows the basic setup of this method, which needs to use the trigger box to match the laser pulses and the camera that will capture the region of interest at the timing of the equal pulses (Neeraj and Lal, 2014). The flow illustrated needed two sequential laser pulses and two matching camera frames to capture the scattering particles in the flow of the test section (Jaan, 2018). This method was able to give the best instantaneous flow structure characteristics with the velocity data from the small size scattering particles in the region of interest. This method has been applied in the study of Dobrev and Massouh, (2012) to investigate the flow characteristics of the Savonius turbine at each rotor angle shown in Figure 2.12. Another PIV flow visualization showed around the H-Darrieus turbine using the Stereo-PIV systems (Rolin and Porté-Agel, 2015) shown in Figure 2.13.

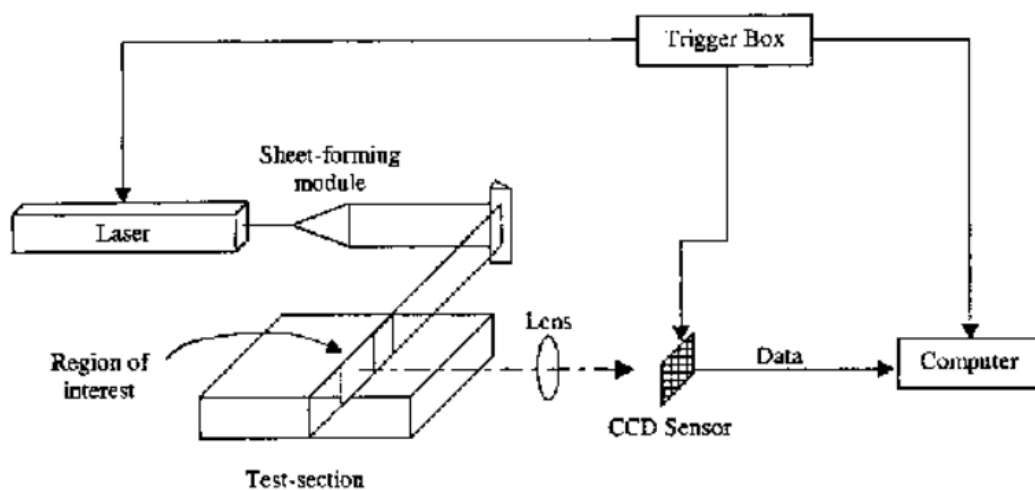


Figure 2.11: The visualization of the set-up of the PIV method with the connected apparatus. (Neeraj and Lal, 2014)

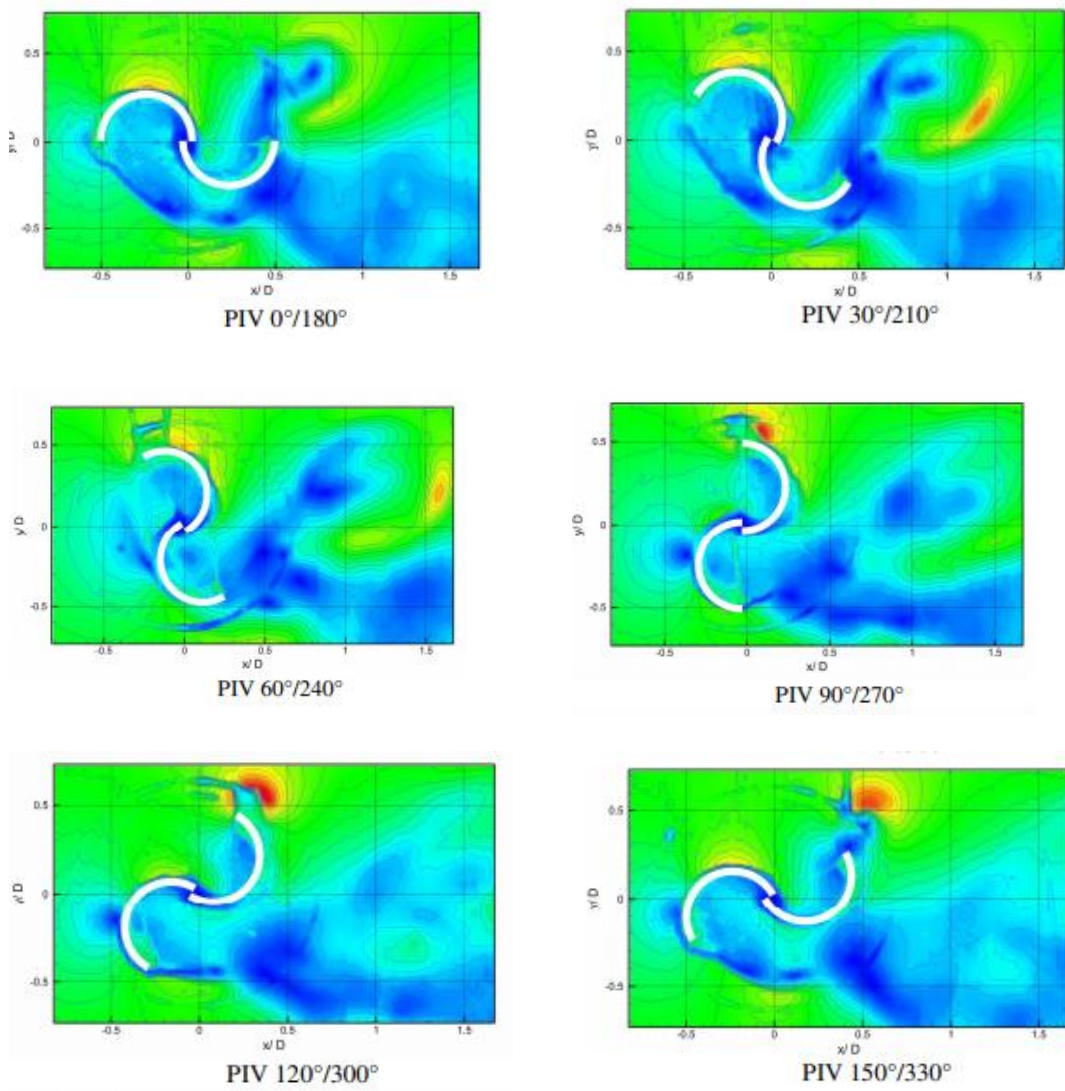


Figure 2.12: The PIV flow visualization at each rotor position (Dobrev and Massouh, 2012).

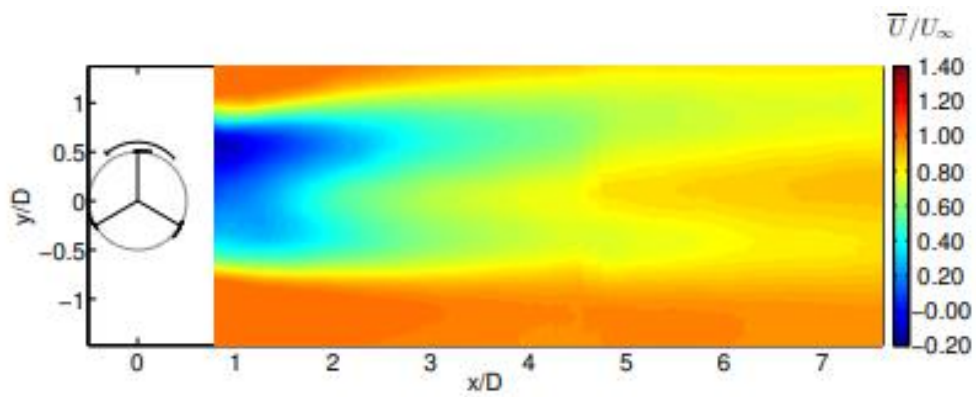


Figure 2.13: The velocity contour of time average stream-wise velocity (Rolin and Porté-Agel, 2015).

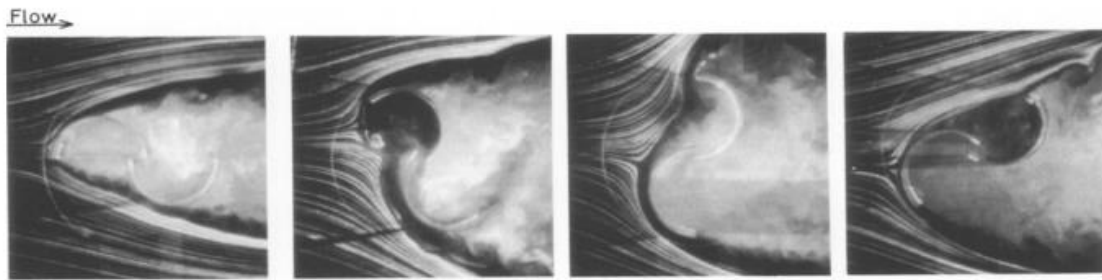
The PIV method is able to collect the qualitative data of the flow around the turbine shown in Figure 2.13. The large velocity deficit at the core in Figure 2.13 and higher turbulence intensity were due to the boundary layer (Rolin and Porté-Agel, 2015). The practicality of using this PIV method in this experiment is low, as high definitions and high-speed cameras equipped with costly lenses are needed to capture the flow velocity and the post-processing process is needed to lower the erroneous vectors (Neeraj and Lal, 2014).

## II. The Smoke Visualization method

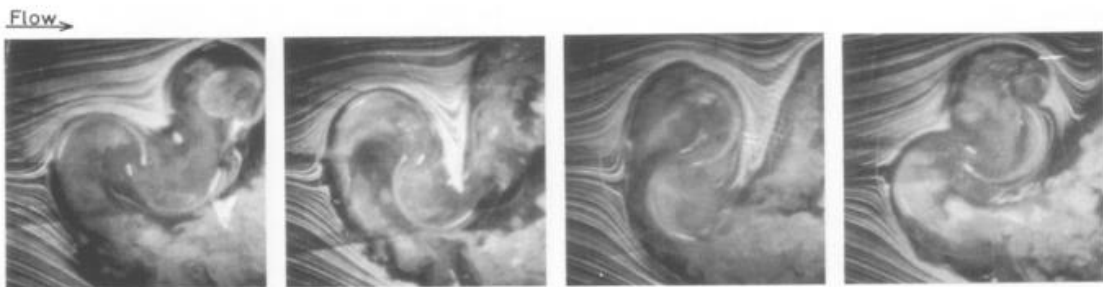
The smoke visualization is divided into two types; smoke generators and smoke wire. Both methods use the same process of heating the smoke liquid, which heats the smoke liquid and transfers it to the smoke wire or smoke rake.

### a. Smoke wire method

This method produces the smoke lines by heating the wire with the oil supplied by the tube and the smoke lines are generated. The smoke wire technique was used by (Fujisawa and Gotoh, 1992) to visualize the flow of the static and rotating Savonius turbine shown in Figure 2.14 around both the static and dynamic Savonius turbine. At a high flow speed, the smoke lines are easily dissipated in the air as the thin smoke lines are produced in the flow (Dol and Kamaruzaman, 2006).



(a)The smoke lines around the static Savonius turbine



(b)The smoke line around the rotating Savonius turbine.

Figure 2.14: The smoke lines around the Savonius turbine (Fujisawa and Gotoh, 1992)

b. Smoke generator method

The smoke generator will heat the nichrome wire inside the generator and the smoke liquid will be fed into the generator to be heated (Shamsuddin and Kamaruddin, 2020). The smoke produced in the generator is then delivered into the feeder that will connect to the smoke rake. The smoke line is produced by each smoke rake in the flow. There are a few smoke liquids that are listed below (Trinder and Jabbal, 2013) and have been tested to visualize the flow in Figure 2.15 from a previous study (Shamsuddin and Kamaruddin, 2020);

Table 2.4: The smoke liquid properties (Trinder and Jabbal, 2013; Shamsuddin and Kamaruddin, 2020)

Smoke type	Advantages	Disadvantages
Tobacco, kerosene	Produce high-quality smoke	Harmful and toxic.
Carbon dioxide	Produce denser smoke	It must be ventilated because it is hazardous in large quantities.
Water-based liquid; Safex oil,	The smoke produced is dense vapour smoke. Non-harmful.	The smoke vapour has the ability to condense back into a liquid



(a) Corn oil



(b) Kerosene

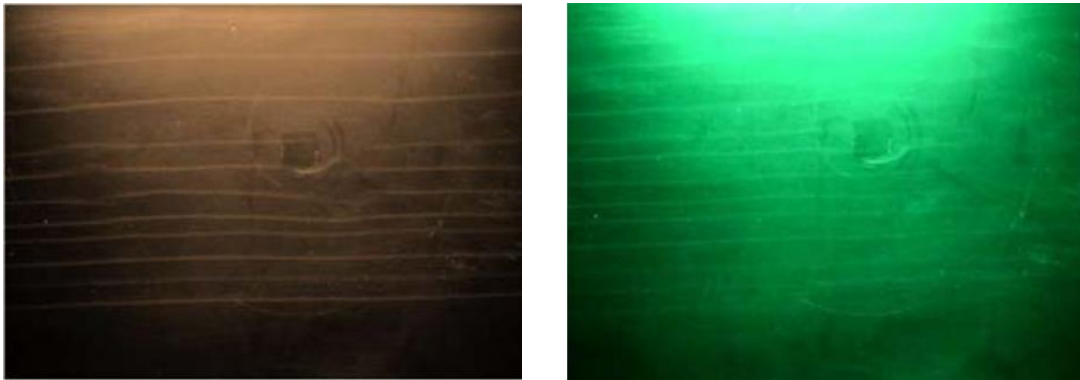


(c) Safex oil

Figure 2.15: The type of smoke oils tested in the wind tunnel (Shamsuddin and Kamaruddin, 2020)



The lighting of the system needs to be reviewed as the lighting is able to show the smoke lines clearly. The halogen light is able to visualize the smoke lines better in comparison to the fluorescent and LED illumination systems, as shown in Figure 2.16 (Shamsuddin and Kamaruddin, 2020).



(a) Fluorescent

(b) LED



(c) Halogen

Figure 2.16: The illumination system's light to show the smoke lines (Shamsuddin and Kamaruddin, 2020).

## 2.4 Relevance of previous literature to the current study

### 2.4.1 Hybrid turbine selection

The hybrid turbine design in this study was finalized with the drag-driven and lift-driven turbine combination consisting of the Savonius turbine and the Darrieus turbine.